TSCFA台灣超臨界流體協會
Taiwan Supercritical Fluid Association

電子報第 186 期

活動訊息

- **第12屆超臨界流體國際研討會暨第21屆超臨界流體技術應用與發展研討會及會員大會**

  時間：2022年**10月28~29日(星期五~六)**

  地點：**集思北科大會議中心億光大樓2樓『感恩廳』**

  https://supergreen2022.conf.tw/

  邀請會員朋友踴躍報名，蒞臨與會交流。

技術專欄

- Efficiency Improvement in Dye-Sensitized Solar Cells by Modify Titanium Dioxide Formation on Supercritical Carbon Dioxide Fluid Synchronous Dyeing

教育訓練班

- (日間班)高壓氣體特定設備操作人員安全衛生教育訓練班 09/26~09/30
- (夜間班)高壓氣體特定設備操作人員安全衛生教育訓練班 10/04~10/16

產業新聞

- SuperGreen2022 國際研討會 10 月 28 日北科大登場

  資料來源：

  https://money.udn.com/money/story/5723/6503962?from=edn_search_result

技術文摘

- Development a novel robust method to enhance the solubility of Oxaprozin as nonsteroidal anti-inflammatory drug based on machine-learning 開發一種基於機器學習的新型穩健方法來提高奧沙普秦作為非甾體抗炎藥的溶解度
- Numerical Study on Proppant Transport in Supercritical Carbon Dioxide under Different Fracture Shapes: Flat, Wedge-Shaped, and Bifurcated 不同斷口形狀下超臨界二氧化碳中支撐劑輸運的數值研究：平面、楔形和分叉
- Retention mechanisms of imidazoline and piperazine-related compounds in non-aqueous hydrophilic interaction and supercritical fluid chromatography based on chemometric design and analysis 基於化學計量學設計和分析的咪唑啉和哌嗪相關化合物在非水親水相互作用和超臨界流體色譜中的保留機制

- SiO_2 synergistic modification of siloxane thickener to improve the viscosity of supercritical CO_2 fracturing fluid 矽氧烷增稠劑 SiO_2 協同改性提高超臨界 CO_2 壓裂液黏度
- Study on the Alteration of Pore Parameters of Shale with Different Natural Fractures under Supercritical Carbon Dioxide Seepage 超臨界二氧化碳滲流下不同天然裂縫頁岩孔隙參數變化研究
- Supercritical Extraction of a Natural Pyrethrin-Rich Extract from *Chrysanthemum Cinerariifolium* Flowers to Be Impregnated into Polypropylene Films Intended for Agriculture Applications *菊花*中富含除蟲菊素的天然提取物的超臨界萃取，以浸漬到用於農業應用的聚丙烯薄膜中
- Supercritical Fluid-Assisted Fabrication of PDA-Coated Poly (L-lactic Acid)/Curcumin Microparticles for Chemo-Photothermal Therapy of Osteosarcoma 超臨界流體輔助製備 PDA 包覆的聚（L-乳酸)/薑黃素微粒用於骨肉瘤的化學光熱治療

台灣超臨界流體協會
電話：(07)355-5706
E-mail：tscfa@mail.mirdc.org.tw

親愛的貴賓 您好:

台灣超臨界流體協會謹訂於民國111年10月28日(星期五)至10月29日(星期六)，假 集思北科大會議中心億光大樓 2 樓『感恩廳』，舉辦「SuperGreen 2022 第12屆超臨界流體國際研討會暨第21屆超臨界流體技術應用與發展研討會」，並於10月29日下午14時舉行111年度會員大會。 恭請

蒞臨指導

SuperGreen 2022國際研討會暨第21屆技術研討會
及年會籌備會主任委員 **謝達仁 王錫福**
副主任委員 **廖盛焜 蘇至善**
台灣超臨界流體協會 全體理監事暨籌備會委員

敬邀

Supergreen 2022 Program

2022/10/24-2022/10/27
<u>Asynchronous Webinar</u> **For all submitted oral and poster presentations** Demo website: https://www.conf.tw/site/order/9999/presentation.aspx?sid=9999&lang=en

說明: 利用非同步平台將所有投稿的口頭報告影片與海報 PDF 檔案上傳其中進行發表，在此段時間內，與會者可隨時上平台瀏覽，並留言進行討論，問答也會即時以 E-mail 傳送通知，類似瀏覽 Youtube 的模式。

2022/10/28 **<u>On-site meeting and live streaming using Cisco Webex</u>** **For plenary and invited speakers from Taiwan** **Room: The Lecture Hall**	
8:30-14:30	Registration
9:10-9:30	Welcome Ceremony
Session 1: Applications of SCF in Taiwan	
9:30-10:05	Plenary lecture 1
10:05-10:30	Invited lecture 1
10:30-10:55	Invited lecture 2
10:55-11:10	Short break
Session 2: Applications of SCF in Taiwan	
11:10-11:35	Invited lecture 3
11:35-12:00	Invited lecture 4
12:00-12:25	Invited lecture 5
12:25-13:30	Lunch (The Lecture Hall)
13:30-14:30	On-site poster presentation (Room 201)
TSCFA annual member meeting **(For TSCFA member only)**	
14:30-17:30	TSCFA annual member meeting
18:00-20:00	Banquet

說明: 實地於北科集思會議中心舉辦實體研討會，並以線上會議軟體 Cisco Webex 同步直播，國際與會者可登入系統參與問答，該日議程包含台灣邀請演講、海報論文實地展示與會員大會。

2022/10/29 **On-line meeting using Cisco Webex** **For international plenary and invited speakers**	
Session 3	
9:00-9:35	Plenary lecture 2
9:35-10:00	Invited lecture 6
10:00-10:25	Invited lecture 7
10:25-10:40	Short break
Session 4	
10:40-11:15	Plenary lecture 3
11:15-11:40	Invited lecture 8
11:40-12:05	Invited lecture 9
12:05-13:30	Lunch time
Session 5	
13:30-14:05	Plenary lecture 4
14:05-14:30	Invited lecture 10
14:30-14:55	Invited lecture 11
14:55-15:20	Invited lecture 12
15:20-15:40	Short break
Session 6	
15:40-16:15	Plenary lecture 5
16:15-16:40	Invited lecture 13
16:40-17:05	Invited lecture 14
17:05-17:30	Invited lecture 15
17:30-17:50	Closing and award ceremony

說明: 純線上研討會，以線上會議軟體 Cisco Webex 進行，所有與會者於線上平台上交流，由所邀請之 14 位國際學者發表演講並討論。

Topics
(1) Physicochemical properties and thermodynamics
(2) Natural products, pharmaceutical and biomedical applications
(3) Reactions, material design and nanotechnology
(4) Processes intensification, CO_2 utilization and industrial applications

第 12 屆超臨界流體國際研討會暨第 21 屆超臨界流體技術應用與發展研討會及會員大會

□ 參加研討會 □參加會員大會 (可重複勾選)

公　司/學校名稱			報名日期	年　月　日
會員別	□團體會員 □個人會員 □學生會員 □非會員		聯絡人	
地　址	□□□		電　話	(　) 分機
姓　名	職　稱	E-mail	活動項目及午餐	
(中)			10/28 □午餐 □晚宴 □不用餐	
(英)				
(中)			10/28 □午餐 □晚宴 □不用餐	
(英)				

活動費用		
	Early Before September 30 2022	Late and On-site After September 30 2022
Online participant	NTD $3,000 (外籍 USD $100)	NTD $4,500 (外籍 USD $150)
Regular participant	NTD $7,500 (外籍 USD $250)	NTD $9,000 (外籍 USD $300)
TSCFA member	NTD $3,000	NTD $4,500
Student	NTD $2,000	NTD $3,000

費用包含：茶點、午餐、晚宴、研討會論文摘要集等，**只參加半天恕不退費**。

※本表如不敷使用，請自行新增，亦可透過會議網站報名，網址：https://supergreen2022.conf.tw/

★上述個人資料本會僅作為此次活動相關服務使用，絕不另作其他用途。特此聲明！

備註：

- 為統計參加人數及確定餐點數量，務必請於**研討會(10/15)**前完成報名手續。
- 報名表請 **e-mail** 至協會，完成報名手續後，本會將製作出席證，出席證於當日報到時領取。
- **研討會地點**：**集思北科大會議中心億光大樓 2 樓感恩廳**。(台北市大安區忠孝東路三段 1 號)
- **晚宴地點**：**福容大飯店台北一館 B1 芙蓉 A 廳**(台北市建國南路一段 266 號)。
- **住宿**：如需住宿者，可參考此次研討會配合飯店，可享有專案費用，請填寫訂房單，由秘書處統計，並代為訂房，亦或直接填寫 google 表單 https://forms.gle/dFKXaSsDMkmUBTZW7。
- 協會聯絡人：吳家瑩小姐，電話：(07)355-5706，E-Mail：tscfa@mail.mirdc.org.tw。
- **付款方式**：

1. 郵局劃撥帳戶：台灣超臨界流體協會；帳號：42221636
2. 銀行匯款戶名：社團法人台灣超臨界流體協會，兆豐國際商銀-港都分行(代碼：017)；帳號：002-09-01847-9 (若以 ATM 轉帳請告知您的姓名及轉帳帳號末五碼以便查對)。
3. 線上付款：可由會議網址報名及繳費 **https://supergreen2022.conf.tw/**。

和苑三井花園飯店 台北忠孝
MGH Mitsui Garden Hotel Taipei Zhongxiao

第12屆超臨界流體國際研討會暨第21屆超臨界流體技術應用與發展研討會及會員大會

訂房單

優惠日期：2022年10月27日(四)至2022年10月28日(五)，共2天

□新增	□修改	□取消
姓名：		性別：□男 □女
入住日期：2022/10/	退房日期：2022/10	天數： 晚
電話/手機：	E-mail/傳真：	
發票抬頭：	發票統編：	
是否開車：	備註：□10/28早餐 □10/29早餐 □不需早餐	

優惠房價表

房型	床型尺寸	間數	房價	小計	坪數及特色
標準大床房	1,630 x 1,970mm		NT$2,600		6.9坪，無浴缸，每層1間
好萊塢雙床房	2小床合併 (2,460 x 2,000mm)		NT$2,700		7.8坪，標準雙床的合併版本，無浴缸
標準雙床房	1,230 x 1,970mm		NT$2,700		7.8坪，無浴缸
總計：NT$_____元(費用內含稅及服務費)					

- ■ 因標準大床房、好萊塢雙床房數量較少，將依回單順序提供，滿房將安排標準雙床房。
- ■ 入住時間：下午3:00，退房時間：中午12:00。
- ■ 請於退房當日將全額款項結清。

客房專屬優惠如下：

- ● 免費使用 2F Lounge和17F大浴場。
- ● 全館免費無線上網服務。
- ● 房內每日4瓶礦泉水。
- ● 美國市佔率第一Serta® 舒達飯店專用床墊。
- ● 免費停車：入住當日下午14:30-退房當日12:30，超過費用為：半小時$30元，當日最高$250元。

- ➢ 早餐為中西日式自助餐，**需另外支付**，金額原價每位$660，本次可提供**優惠價$500**。(至多2位)
- ➢ 當天臨時變更、取消房間費用不予退還，以入住第一晚房費計算。

和苑三井花園飯店 MGH Mitsui Garden Hotel Taipei Zhongxiao
10652 台北市大安區忠孝東路三段30號
TEL (02)2781-1131 FAX (02)2781-1130 https://www.gardenhotels.co.jp/taipei-zhongxiao/tw/

技術專欄

Efficiency Improvement in Dye-Sensitized Solar Cells by Modify Titanium Dioxide Formation on Supercritical Carbon Dioxide Fluid Synchronous Dyeing

Shen-Kung Liao[1*], Jin-yu Ruan[1], Chie-Hao Chao, Chih-Hsun Liao[2]

[1]Department of Fiber and Composite Materials, Feng Chia University, Taichung, Taiwan
[2]SCH Electronics Cooperative Limited, Taiwan
tel +886-4-24517250ext3435, fax +886-4-24514625, e-mail：skliao@ fcu.edu.tw

ABSTRACT:

In this study, the dye sensitized solar cells (DSSC) were assembled by using natural dyes extracted from roselle and red phoenix as sensitizer coated fluorine-doped tin dioxide substrate (FTO) plate used a counter electrode for nanocrystalline TiO_2. We investigated the formation of modified titanium dioxide on dye-sensitized solar cells by simultaneous dyeing with supercritical carbon dioxide fluid. The photoelectrode is made of compact layer and scattering layer. Supercritical carbon dioxide fluid extracted natural dyestuff and synchronous dyed photoelectric. The photoelectric conversion efficiency is the best at the dyeing parameters of 3000 psi, 50 ºC, and 30 minutes. Experimental results show that adding a scattering layer to the compact layer can improve the conversion efficiency. SEM can observe that the polyethylene glycol-added scattering layer has more pore structures in which improves the electrode's ability to capture sunlight. The conversion efficiency of 0.13% can be obtained by using 9:1 mixed dyes of anthocyanin and chlorophyll. The photoelectric conversion efficiency with the P25/R-type/PEG scattering layer is about 30% higher than that of a single compact layer. Finally the paper proposes a schematic diagram of the dye-sensitized solar cell.

Keywords: Synchronous Dyeing, Dye-sensitized, Supercritical fluid, Anthocyanins, Chlorophyll, DSSC.

1. INTRODUCTION

Dye-sensitized solar cells (DSSCs) are the process of sensitizing the wavelength of visible light into electrical energy. DSSCs have the advantages of environmental protection and low manufacturing costs, as well as their added value in the product and commercial application, so it has always been a topic of great interest to related researchers. The performance of the DSSCs mainly depends on a dye used as sensitizer. The absorption spectrum of the dye and the titanium dioxide photoelectrode of formation are important that determining the conversion efficiency of DSSCs, as shown figure 1 model of dye sensitized solar cells.[1-3] The first DSSCs was designed in 1976 in Japan by Tsubomura, who found that porous zinc

oxide of photoelectric, but the research are neglected because low efficiency. Until 1991 in Switzerland, Gratzel used nanostructures as photoelectric to adsorbing the dye.[4,5] The nanostructures DSSCs the efficiency higher than before and the manufacturing cost are lower than traditional silicon solar cells.

Because titanium dioxide usually only absorbs ultraviolet light, it is necessary to effectively use sunlight in dye-sensitized solar cells. In addition to modifying the titanium dioxide itself, another method is to immerse the dye molecules on the metal oxide by soaking in a chemical solution. Judy N. Hart et al. showed that the barrier layer can improve the conversion efficiency of the battery. The more barrier layers, the higher the battery efficiency. In 2006, Hore S et al. pointed out that adding a scattering layer can effectively improve the conversion efficiency of the battery. In the study up to 80% increase in current density was observed due to inclusion of scattering layers. In 2010, Jinho Chae et al. combined nano-scale gallium with titanium dioxide to make a photoelectrode. The results show that the conversion efficiency of the photoelectrode combined with gallium is about 4.57% higher than that of the pure titanium dioxide photoelectrode.[6-8] In 2012 Niu Huang et al. used titanium tetrachloride to treat zinc oxide photoelectrode. The photoelectrode can improve the adsorption of dyes and form a good electron transport film with a conversion efficiency of 6.39%. In the same year, Curtiss S et al. used the RF-sputtering method and the sol-gel method to prepare the compact layer, which can improve the contact between the conductive film and the electrode, and the conversion efficiency of the two methods were increased by about 18.9% and 25.3%, respectively.[9,10]

Gases and liquids become supercritical fluids when they are compressed and heated above their critical pressure and temperature. In this state these supercritical fluids exhibit properties between those of typical gases and liquids. Compared with liquids, the density and viscosity of supercritical fluids are lower, but diffusion in these materials is greater. Hence, supercritical fluids are widely used in chemical extraction, reactions, polymerization, chromatography, and impregnation of desired additives into various materials. Austrian scholar Marr and German scholar Werner reviewed related literature publication and technical conditions of using supercritical fluid in extraction processing, and proposed that the phase behavior of supercritical fluid dissolved solute under different PVT (P: pressure, V: volume, T: temperature) conditions is the key factor influencing the extraction effect. They argued that the important factors, such as phase behavior and solubility of solute in supercritical fluid, could be estimated by using the equation of state.[11-13] In this paper, we use supercritical carbon dioxide dyeing technology instead of impregnation as a facile process for fabrication dye-sensitized solar cells using anthocyanin/chlorophyll into titanium dioxide as the photoelectrode. The DSSCs photoelectrode is currently impregnation and require for up to twenty hours or more, so the adsorption isn't satisfactory by impregnation. We use the supercritical CO_2 fluid viscosity and diffusion, the adsorption of titanium dioxide could decrease the time to dyed nanocrystalline titanium dioxide photo-electrodes and avoiding

prolonged exposure to photosensitive dye into the air. Thus we expect supercritical fluid dyeing way improves efficiency of DSSCs and achieve zero pollution.

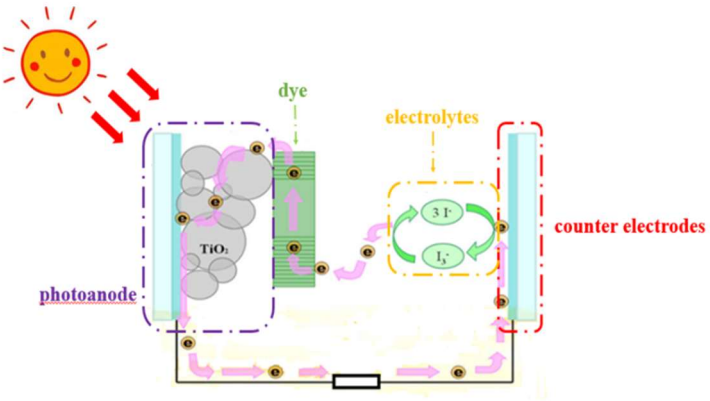

Figure 1. Schematic diagram of dye sensitized solar cells

2. EXPERIMENTAL

2.1 Titanium dioxide compact layer

In this experiment, titanium isopropoxide, ethanol, nitric acid and deionized water were used in molar ratios of titanium isopropoxide: ethanol: nitric acid: deionized water by1:15:3:2, stirred at room temperature for 24 hours to prepare a sol gel precursor firstly. Add 0.1 mL of acetone as a dispersant to uniformly disperse the resulting sol-gel. After the reaction is completed, the sol-gel solution is spin-coated on FTO to form a titanium dioxide film, which is passed through a vacuum oven Drying at 70 ℃ and then sintering at 500 ℃ in a high-temperature furnace to obtain a compact layer of titanium dioxide. Second Degussa P25 titanium dioxide, ethanol and deionized water were made into titanium dioxide slurry with a weight percentage of 1:2:2, and 0.1 mL of acetone was added as a dispersant. The titanium dioxide slurry is stirred for 12 hours with an electromagnetic heating stirrer, and then spin-coated on the FTO substrate to form a thin film. After the thin film is dried, it is sintered in a high-temperature furnace to obtain the battery compact layer.

2.2 Light scattering layer

Use commercial titanium dioxide, polyethylene glycol, ethanol and deionized water at a weight percentage of 1:1:3:3 and add 0.1 mL of acetone to prepare a titanium dioxide slurry, which uses Rutile-type and Degussa P25 respectively. Two kinds of titanium dioxide R-type and Degussa P25 were obtained from Echo Chemical Co, Taiwan. As a material for preparing the slurry, the Rutile-type is a white powder with a purity of 99.9% in Titanium(IV) oxide rutile form and a particle size range of 200-400 nm. The other Degussa P25 is a white powder with a particle size of 21 nm of Titanium(IV) oxide powder. The titanium dioxide slurry was stirred with an electromagnetic heating stirrer for 12 hours, spin-coated on the dye adsorption layer, dried and sintered at a high temperature to obtain the light scattering layer of the electrode. The flow chart is shown in Figure 2. Four scattering layers of R-type, R-type/PEG, P25/PEG, and P25/R-type/PEG are produced according to different matching parameters.

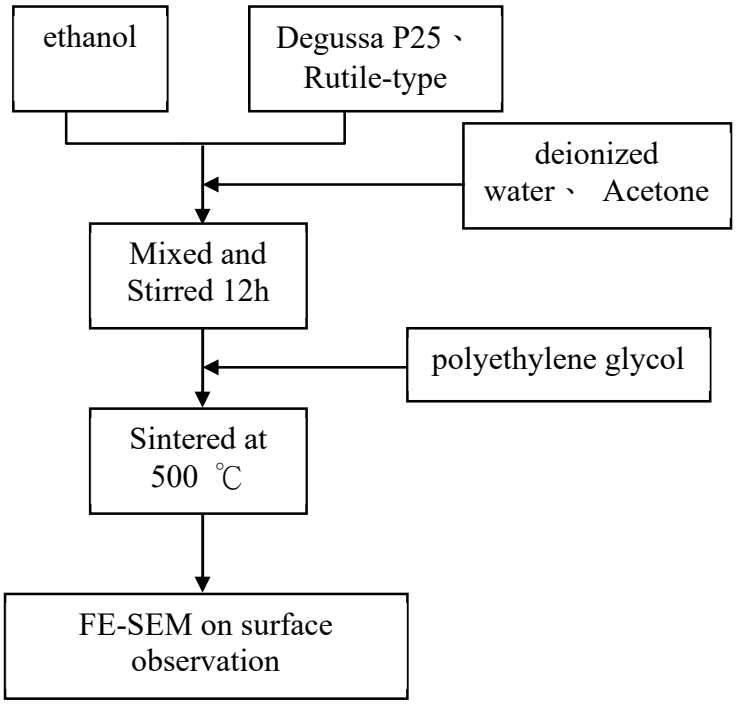

Figure 2. Flow chart of light scattering layer production

2.3 Dye extraction and simultaneous dyeing

The development of solar green renewable energy, and has many advantages are great attention.[14,15] Dye-sensitized solar cells use cheap and easy-to-obtain glass as the base material and are coated with conductive materials, combined with dye molecules and nano-level metal oxide semiconductor powder, which can absorb sunlight and convert it into electrical energy. The photoelectrode is prepared by using supercritical carbon dioxide fluid to utilize its high density and high diffusivity to achieve high-efficiency dye extraction and photoelectrode simultaneous dyeing to shorten the manufacturing process. The dye-sensitized solar cell still maintains the original or even better photoelectric conversion efficiency.

Chlorophyll is a fat-soluble natural pigment that is widely present in plant leaves in nature. Its basic structure is mainly composed of four pyrroles, forming a macrocyclic compound with conjugated double bonds called porphyrin. It is called pyrrolidin. Chlorophyll is a magnesium porphyrin derivative. It consists of four nitrogen atoms chelating a magnesium ion and has the function of absorbing light energy. The porphyrin ring has a special long chain of carbon and hydrogen, one of which is a long chain of phytol, which is called phytol. Figure 3 shows the structure of chlorophyll. Chlorophyll is used as a sensitizer for dye-sensitized solar cells, and its bonding method is shown in Figure 4.[16] Diagram of titanium dioxide and anthocyanins bonding scheme was shown and our early studies too.[3,17]

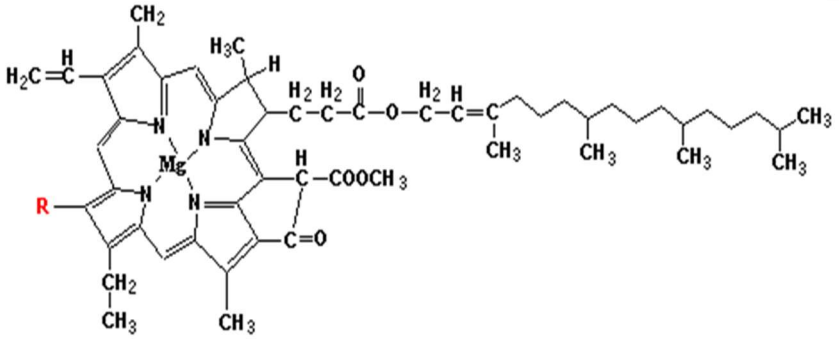

Figure 3. Structure of chlorophyll.

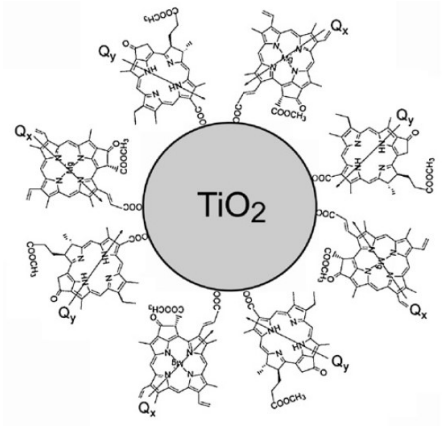

Figure 4. Diagram of titanium dioxide and chlorophyll bonding scheme.

Using titanium dioxide, polyethylene glycol, ethanol and deionized water at a weight percentage of 1: 1: 3: 3 and adding 0.1 mL of acetylacetone to form titanium dioxide slurry, in this case two titanium dioxide R-type and Degussa P25 were used as the material for the preparation of the slurry. The titanium dioxide slurry was stirred for 12 hours with an electromagnetic heating stirrer, spin coating on the compact layer after drying and high temperature sintering to get the electrode light scattering layer. The R-type, R-type / PEG, P25 / PEG, P25 / R-type / PEG four kinds of scattering layers were prepared according to different parameters.

3. RESULT AND DISCUSSION

3.1 Particle Size analyses

The particle size analysis of sol-gel titanium dioxide is presented in Figure 5. The particles are distributed from 3 nm to 55 nm, mainly in the range of 3.79-6.80 nm. The Table 1 is analysis volume results of sol-gel titanium dioxide, the average particle size of the titanium dioxide particles is 6.3 nm, the particle size is less than 10 nm, but the volume percentage is below 2%. The size of the sol-gel titanium dioxide particles is uniform and the particle size difference is not significant.

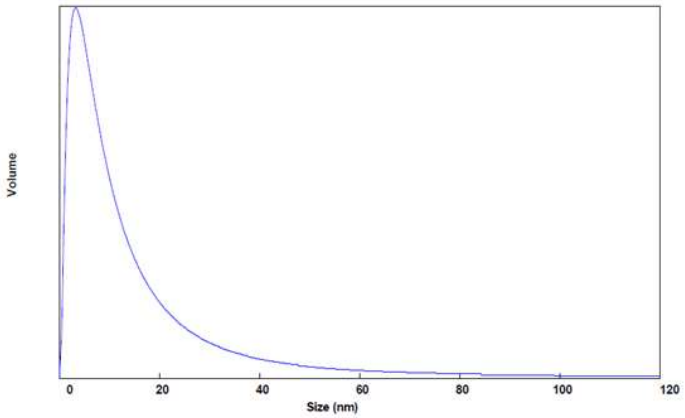

Figure 5. The particle size distribution of sol-gel titanium dioxide

Table 1. The particle size of sol - gel titanium dioxide from volume results summary

Angle	Calculated Results				
	Size (nm)	% amt (nm)	Std.Dev (nm)	Mean Size (nm)	% Dust
90.0°	4.4	87.25	0.8	6.3	0.000
	19.5	12.75	7.6		

3.2 Powder XRD analysis

The crystalline phase of TiO2 nanoparticles were analyzed by X-ray diffraction (XRD type MXP3) measurement using target material: Cu, wavelength: 1.5405 nm, filter: Ni, voltage: 30KV, current 20mA, scanning angle: 5° -70° , analyze the crystal form and crystal strength of the titanium dioxide film to determine the crystal form of the sample. Figure 6 shows the powder XRD pattern of as- prepared TiO2 nano-particles and the presence of sharp diffraction peaks in the XRD confirm that products are highly crystalline. Shown on Figure 6(a), XRD spectra of titanium dioxide compact layer that a strong diffraction peak at 2θ = 25.045° and the secondary diffraction peaks at 2θ = 36.083° ,39.189° ,41.239° ,44.057 ° ,54.321° ,56.632 ° and 69.007° which is the diffraction peak of rutile(110). In addition, a smaller diffraction peak appears at 2θ = 27.215° ,which is the main diffraction peak of rutile(110), and the secondary diffraction peak at 2θ = 35.925° is also consistent with the reference to the characteristics of rutile titanium dioxide peak. The peaks of anatase(101) and rutile(110) appear in the XRD pattern. The titanium dioxide produced in this experiment is mainly composed of anatase phase and trace rutile phase.

Degussa P25 is composed of anatase phase and rutile phase composed of titanium dioxide, the weight ratio of 71 to 29, as shown in Figure 6(b), there is a strong diffraction peak at 2θ = 25.250° ,and followed by 2θ = 38.471° ,48.010° ,53.917° ,55.024° and 62.702° which is the diffraction peak of anatase(101). In addition, the main diffraction peak of rutile(110) is shown at 2θ = 27.410° ,followed by 2θ = 36.046° and 68.905° .It can be proved to the experiment used P25 titanium dioxide for the anatase phase and a small amount of rutile phase.

R-type titanium dioxide is almost composed of rutile phase, as shown in Figure. X(c), that a strong diffraction peak at 2θ = 27.410° ,which is the main diffraction peak of rutile(110). The secondary diffraction peaks at 2θ = 36.083° ,39.189° ,41.239° ,44.057° ,54.321° ,56.632 ° and 69.007° are in line with the rutile phase characteristic peaks mentioned in the literature.[18]

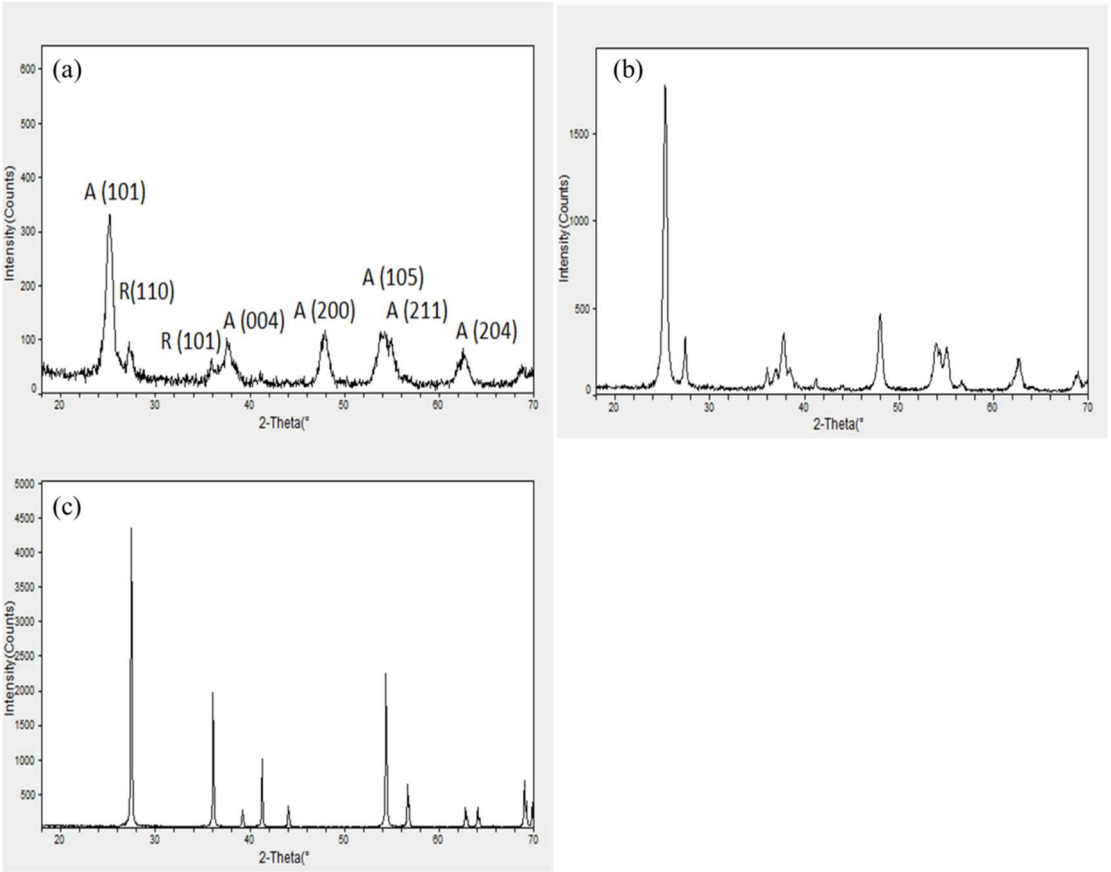

Figure 6. XRD spectra of (a) Titanium dioxide compact layer (b) P25 Titanium dioxide (c) R-type Titanium dioxide

3.3 Scanning Electron Microscope analysis of the electrode surface

In the study we investigated the modified of photoelectrode was made with compact layer and scattering layer. In this part, analysis of the electrode surface from scanning electron microscope analysis.

(1) Compact layer: The SEM of the sol-gel titanium dioxide compact layer is shown in Figure 7. These micrographs indicate that the surface of titanium dioxide particle size is uniform. The particle size of the compact layer after high temperature sintering is about 5 nm, and a few titanium dioxide particles larger than 5 nm are also smaller than 10 nm, which is consistent with the results of the aforementioned particle analysis, and the structure is shown in Figure 8 which is schematic diagram of titanium dioxide compact layer.

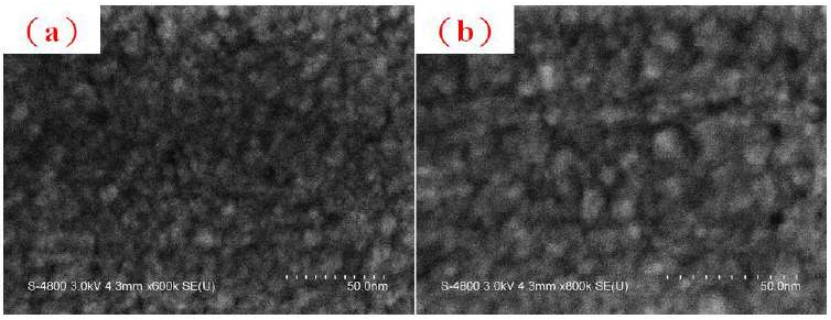

Figure 7. Scanning electron micrograph (SEM) of the sol-gel titanium dioxide compact layer. Magnification at (a) 600 k (b) 800 k

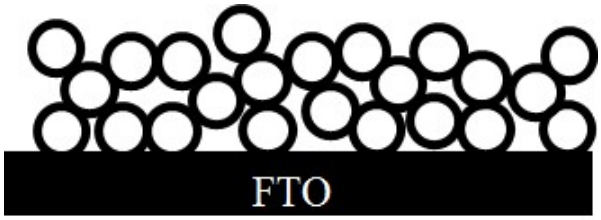

Figure 8. Schematic diagram of titanium dioxide compact layer

In order to increase the thickness of the compact layer, it is expected that more photoelectric dyes can be adsorbed, so this experiment increases the number of coatings. Figure 9 shows the compact layer repeated one to four times. Obviously, the surface of the coated single compact layer is completely smooth with only a few parts producing small cracks. The surface of the double-layer compact layer is severely cracked and split into small uniform pieces. The surface of the compact layer with more than three layers is split into massive titanium dioxide of different sizes, and even peeling. According to the experimental results, it could be found that as the number of compact layers increases the cracks on the surface become more obvious. And the peeled off massive titanium dioxide will destroy the overall structure of the compact layer. Unfortunately these cannot improve the conversion efficiency of the photovoltaic cell when we repeated coating of the compact layer. Even greatly reduce its conversion efficiency.

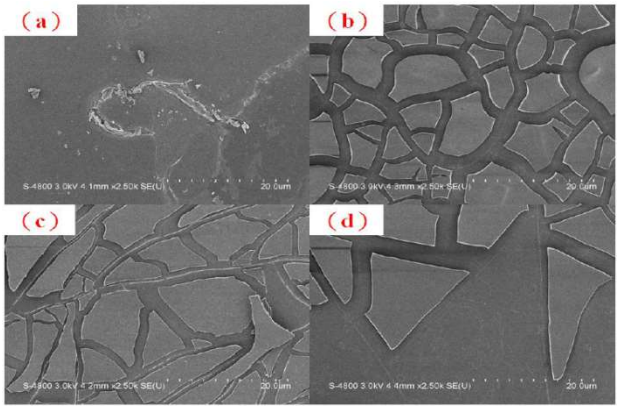

Figure 9. Scanning electron micrograph (SEM) of the compact layers (a) monolayer (b) bilayer (c) three layers (d) four layers. Magnification at 2.5 k.

(2) Scattering layer: The SEM of the R-type, R-type/PEG, P25/PEG, P25/R-type/PEG four kinds of scattering layers in Figure 10. As shown in Figure 10(a), the scattering layers of R-type found extensive aggregation of titanium dioxide which have void around 500 nm. The void structure leads to difficulty of electronic transmission and reduce the DSSCs conversion efficiency. Figure 10(b) shows the scattering layers of R-type/PEG, which have void around 100 nm. In the process of adding polyethylene glycol, it leads titanium dioxide to reducing aggregated. Figure 10(c) shows the scattering layers of P25/PEG. The particle size of P25 titanium dioxide is smaller than R-type. Therefore, photoelectrodes of P25/PEG scattering layers have void less than R-type/PEG. Figure 10(d) shows the scattering layers of P25/R-type/PEG. We can find R-type and P25 titanium dioxide are evenly mixed. Even though the scattering layers have voided, which filled up with P25 titanium dioxide? The P25/R-type/PEG photoelectrodes is best structure of scattering layers. It is shown that this structure is due to multiple refraction of light. The structure is shown in Figure 11 which is schematic diagram of titanium dioxide scattering layer. SEM can observe that the polyethylene glycol-added scattering layer has more pore structures. These pores and irregular surface patterns enable more sunlight to be scattered in which improves the electrode's ability to capture sunlight.

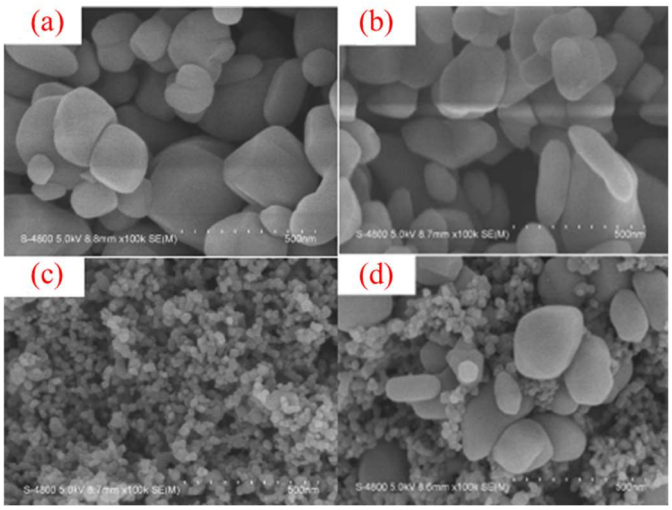

Figure 10. Scanning electron micrograph (SEM) of the scattering layers. (a)R-type (b)R-type/PEG (c) P25/PEG (d) P25/R-type/PEG. Magnification at 100 k.

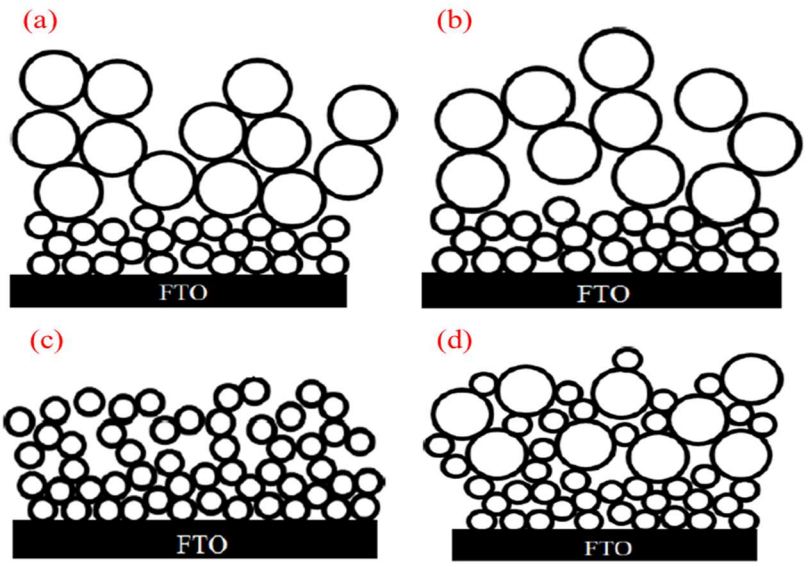

Figure 11. Diagram of different titanium dioxide scattering layers schemme. (a)R-type (b)R-type/PEG (c) P25/PEG (d) P25/R-type/PEG.

3.4 I-V testing of photocells

The TiO2-coated FTO glass substrates were thermally treated using supercritical carbon dioxide fluid synchronous dyeing method in this study. In the experiment, natural dyes were used to extract anthocyanins and chlorophylls, and supercritical carbon dioxide fluid was used to dye natural dye-sensitized solar cells. Electrochemical instruments test different extraction and dyeing conditions to obtain the best conversion efficiency parameters. From the experimental results, we can obtain natural dyes with a conversion efficiency of 0.05~ 0.07 % on anthocyanins and chlorophyll natural dyes with a conversion efficiency of 0.04~0.08% in Figure 12. The use of supercritical carbon dioxide fluid extraction and simultaneous dyeing is compared with traditional solvent extraction dyeing. The latter takes 105 minutes, but the former can achieve the same effect in only 30 minutes, and there is no problem of organic solvent pollution. It can be clearly seen that the use of supercritical fluid as a medium can significantly shorten the material extraction and dyeing time. In this experiment, the effect of placing the scattering layer is obvious.The main reason is that supercritical carbon dioxide fluid has the characteristics of low surface tension, low viscosity and high diffusivity, so it can be easily removed from plants and to achieve the purpose of dyeing.

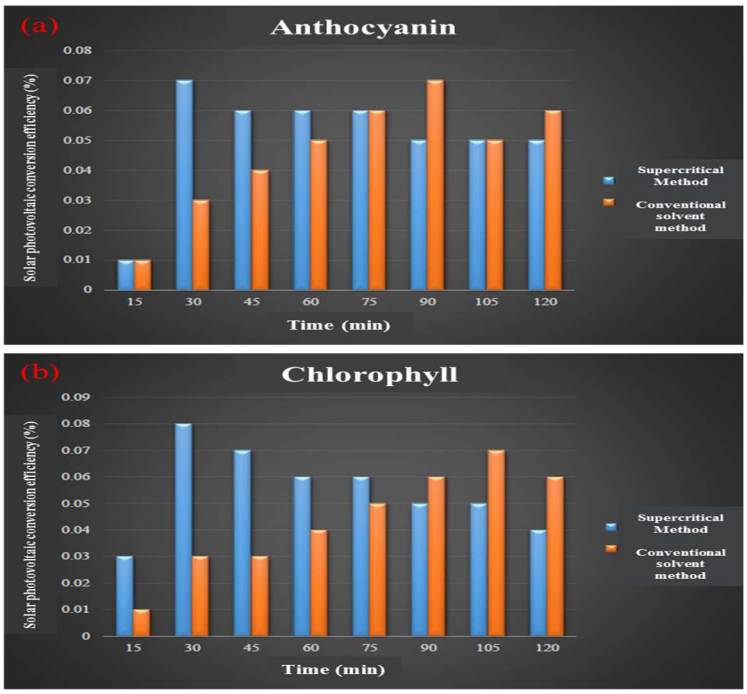

Figure 12. Effect of dyeing time on solar photoelectric conversion efficiency by solvent method and supercritical method. (a) anthocyanin (b)chlorophyll

In order to increase the availability of dye-sensitized solar cells, this study also considered cocktail dyes mixed with anthocyanins and chlorophyll to improve the thermal stability of natural dyes. Table 2 shows roselle and red phoenix as the cocktail dye mixing codes used in the experiment. The 9:1 cocktail dye of anthocyanin and chlorophyll showed the best conversion efficiency of 0.13% in Figure 13. Because the thermal stability of chlorophyll is worse than that of anthocyanin, anthocyanin is used as a protective agent to improve the conversion efficiency.

Supercritical carbon dioxide fluid synchronous dyeing procedure is used at the pressure 3000 psi with 30 minutes. The anthocyanin reaches the best photoelectric conversion efficiency of 0.10% and the chlorophyll is 0.08%. The cocktail dye mixed with anthocyanin and chlorophyll by weight ratio of 9:1 can effectively improve the photoelectric conversion efficiency of the battery to 0.13% by supercritical fluid treatment at 50 ℃, which is improved by 62.5% and 55.6% compared with anthocyanin and chlorophyll dyes. And after improvement, the light half-decay test can reach about 3.6 hours, shown on Figure 14. Experimental results show that the use of cocktail dyes can effectively improve the photoelectric conversion efficiency of the battery and has better stability of descent. Figure 15 shows that decline curve of conversion efficiency with different layers. We can find R-type and R-type/PEG scattering photoelectric conversion efficiency curve are even lower than that of pure dye adsorption layer. Because R-type and R-type/PEG scattering layers affected by rutile titanium dioxide that can't achieve good electron transport. P25 /R-type/PEG scattering layer showed good photoelectric conversion efficiency at the initial stage because the R-type was homogeneously mixed with P25 titanium dioxide in the scattering layer and had good contact to produce similar synergistic effect. That is meaning that it becomes necessary to include a light scattering layer such that the lower photon conversion due to compact layer could be compensated. [7,19] In this experiment, the effect of placing the scattering layer is obvious. Finally the paper proposes a schematic diagram of the dye-sensitized solar cell, as

shown in figure 16.

Table 2. Cocktail dyestuff mixed code

Cocktail dyestuff mixed	Dye weight ratio	
	Chlorophyll	Anthocyanin
CA91	9	1
CA73	7	3
CA55	5	5
CA37	3	7
CA19	1	9

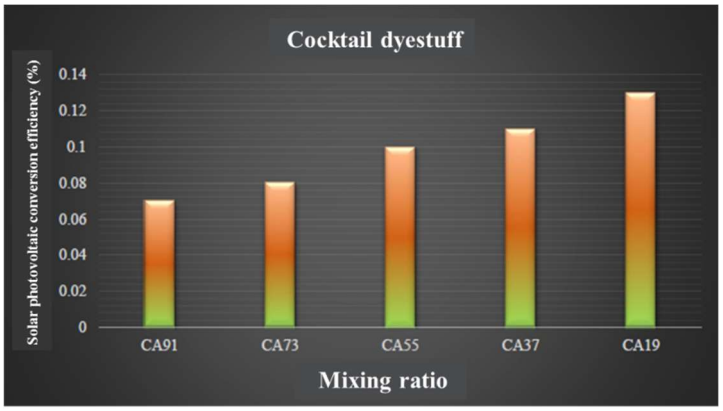

Figure 13. The conversion efficiency of cocktail dyestuff mixed by supercritical carbon dioxide fluid synchronous dyeing.

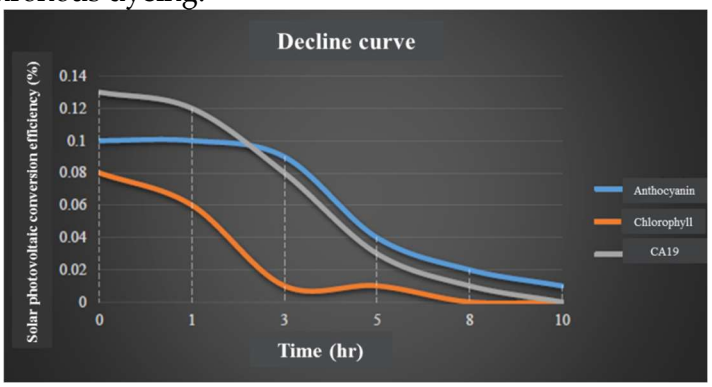

Figure 14. The decline curve of conversion efficiency at anthocyanin, chlorophyll and cocktail CA19

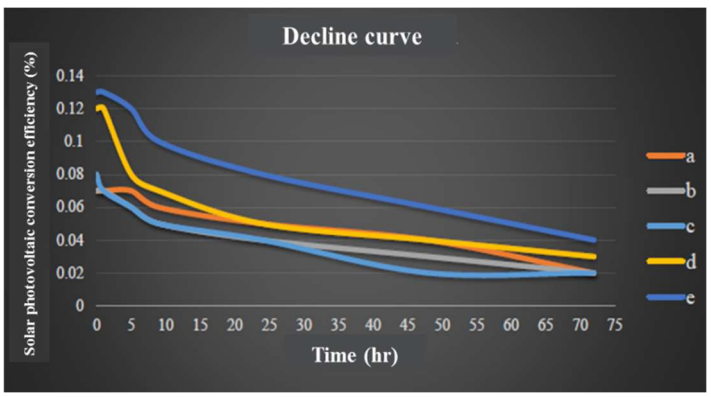

Figure 15. The decline curve of conversion efficiency (a) compact layer, and 4 kinds of scattering layer (b) R-type (c) R-type/PEG (d) P25/PEG (e) P25/R-type/PEG

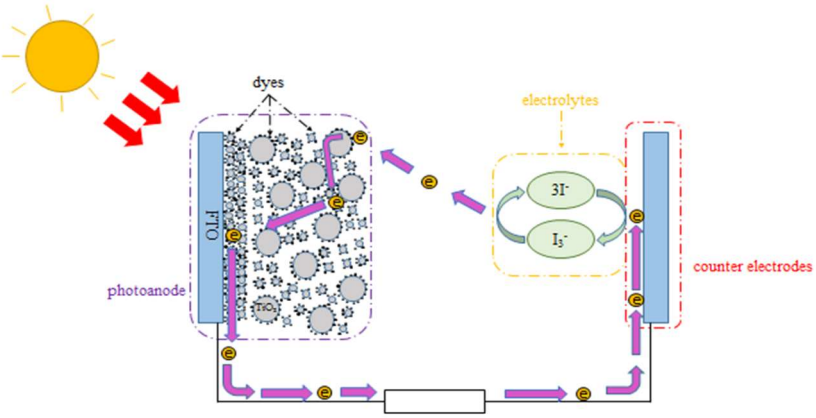

Figure 16. Model of schematic diagram on dye sensitized solar cells

CONCLUSIONS

Dye-sensitized solar cells (DSSCs) belong to the group of thin-film solar cells which have been under extensive research for more than three decades due to their low cost, simple preparation methodology, low toxicity and ease of production. In conclusion, DSSCs offers an efficient and easily implemented technology for future energy supply. Compared to conventional silicon solar cells, it provides comparable the photoelectric conversion efficiency at low material and manufacturing costs. This Paper study provided the experimental evidence that supercritical carbon dioxide fluid synchronous dyeing enhances cocktail dyes mixed with anthocyanins and chlorophyll to improve the thermal stability of DSSCs. The supercritical mechanism is a green environmental indicator. Using its high density and high diffusivity to make dye-sensitized solar cells can effectively shorten the manufacturing process and achieve high efficiency dyes. The extraction and the photoelectrode are dyed simultaneously to reduce the interference of external factors, thereby improving the photoelectric conversion efficiency of the battery. Compared with the traditional solvent method, the use of supercritical carbon dioxide fluid to extract the dye and the simultaneous dyeing of the photoelectrode reduces the manufacturing process while the battery still maintains the original or even better photoelectric conversion efficiency. At the same time, SEM can observe that the polyethylene glycol-added scattering layer has more pore structures. These pores and irregular surface patterns enable more sunlight to be scattered, which improves the electrode's ability to capture sunlight. Effectively improve the photoelectric conversion efficiency of the battery. Finally, the paper proposes a schematic diagram of the dye-sensitized solar cell including compact layer and scattering layer.

Acknowledgments

The authors are grateful to the National Science Council in Taiwan for financial support.

REFERENCES

[1] GiuseppeCalogero, Gaetano DiMarco., (2008) Red Sicilian orange and purple eggplant fruits as

natural sensitizers for dye-sensitized solar cells, Sol. Energy Mater. Sol. Cells, Vol.92, 1341-1346. https://doi.org/10.1016/j.solmat.2008.05.007
[2] Shen-Kung Liao,Yuan-Hsu Chang,Chung-Tse Wu,Yan-Rong Lai,Wei-Yu Chen., (2017) Fabrication of anthocyanin-sensitized nanocrystalline titanium dioxide solar cells using supercritical carbon dioxide, Journal of CO_2 Utilization, Vol.21, 513-520. DOI: 10.1016/j.jcou.2017.07.006
[3] Jiawei Gong, K.Sumathy, Qiquan Qiao, Zhengping Zhou., (2017) Review on dye-sensitized solar cells (DSSCs): Advanced techniques and research trends, Renewable and Sustainable Energy Reviews, Vol.68(1), 234-246. https://doi.org/10.1016/j.rser.2016.09.097
[4] Tsubomura, H., Matsumura, M., Nomura, Y., Amamiya, T., (1976) Dye sensitized zinc oxide/aqueous electrolyte/platinum photocell, Nature, Vol. 261, p.402-403. https://www.nature.com/articles/261402a0
[5] Grätzel M., O'Regan B., (1991) A low-cost, high-efficiency solar cell based on dye- sensitized colloidal TiO_2 films, Nature, Vol. 353, 737-740. https://www.nature.com/articles/353737a0
[6] Judy N. Hart, David Menzies, Yi-Bing Cheng, George P., Simon, Leone Spiccia., (2006) TiO_2 sol–

gel blocking layers for dye-sensitized solar cells, Comptes Rendus Chimie, Vol. 9(5-6), 622–626.

https://doi.org/10.1016/j.crci.2005.02.052

[7] Hore S., Vetter C., Kern R., Smit H., Hinsch A.,(2006) Influence of scattering layers on efficiency of dye-sensitized solar cells, Solar Energy Materials & Solar Cells, Vol.90(9), 1176–1188. DOI:10.1016/j.solmat.2005.07.002
[8] Jinho Chae, Dong Young Kim, Sujung Kim, Misook Kang., (2010) Photovoltaic efficiency on dye-sensitized solar cells (DSSC) assembled using Ga-incorporated TiO_2 materials, Journal of Industrial and Engineering Chemistry, Vol.16(6), 906–911. DOI:10.1016/j.jiec.2010.09.012
[9] Niu Huang, Yumin Liu, Tao Peng, Xiaohua Sun, Bobby Sebo, Qidong Tai, Hao Hu, Bolei Chen, Shi-shang Guo, Xingzhong Zhao., (2012) Synergistic effects of ZnO compact layer and TiCl4 post-treatment for dye-sensitized solar cells, Journal of Power Sources, Vol.204, 257- 264. DOI:10.1016/j.jpowsour.2011.12.027
[10] Curtiss S. Kovash Jr., James D. Hoefelmeyer, Brian A. Logue., (2012) TiO_2 compact layers prepared by low temperature colloidal synthesis and deposition for high performance dye-sensitized solar cells, Electrochimica Acta, Vol.67, 18-23. DOI:10.1016/j.electacta.2012.01.092
[11] R. Marr and T. Gamse., (2000) Use of Supercritical Fluids for Different Processes Including New Developments: A Review, *Chemical Engineering and Processing*, Vol.39(1), 19-28. DOI:10.1016/S0255-2701(99)00070-7
[12] W. H. Hauthal., (2001) Advances with Supercritical Fluids (Review), *Chemosphere*, Vol. 43(1), 123-135. DOI:10.1016/S0045-6535(00)00332-5
[13]Shen-kung Liao & Chang Pi-Shiun., (2012) Literatures on Dyeing Technique of Supercritical Fluid Carbon Dioxide" American Journal of Analytical Chemistry, Vol.3(12A),923-930.
DOI: 10.4236/ajac.2012.312A122
[14] Giuseppe Calogero, Gaetano Di Marco, (2008) Red Sicilian orange and purple eggplant fruits as natural sensitizers for dye-sensitized solar cells, Solar Energy Materials & Solar Cells, Vol.92(11), 1341-1346. https://doi.org/10.1016/j.solmat.2008.05.007
[15] Jung-Kun Lee, Mengji Yang, (2011) Progress in light harvesting and charge injection of dye-sensitized solar cells, Materials Science and Engineering, Vol.176(15), 1142–1160. DOI:10.1016/j.mseb.2011.06.018
[16] Xiao-Feng Wang, Yasushi Koyama, Osamu Kitao, Yuji Wada, Shin-ich Sasaki, Hitoshi Tamiaki,

Haoshen Zhou.,(2010) Significant enhancement in the power-conversion efficiency of chlorophyll co-sensitized solar cells by mimicking the principles of natural photosynthetic light-harvesting complexes, Biosensors and Bioelectronics, Vol.25(8), 1970-1976. https://doi.org/10.1016/j.bios.2010.01.015

[17]T.S.Senthil, N.Muthukumarasamy, Dhayalan Velauthapillai, S.Agilan, M.Thambidurai, R.Balasundaraprabhu.,(2011) Natural dye (cyanidin 3-O-glucoside) sensitized nanocrystalline TiO2 solar cell fabricated using liquid electrolyte/quasi-solid-state polymer electrolyte, Renewable Energy, Vol.36(9), 2484-2488. DOI:10.1016/j.renene.2011.01.031

[18]P. Sanjay, K. Deepa, J. Madhavan, S. Senthil.,(2018) Fabrication of DSSC with Nanostructured TiO2 Photoanode and Natural Dye Sensitizer extracted from fruits of Phyllanthus reticulatus, International Journal of Scientific Research in Scienceand Technology, Vol.4(5), 437-443. https://www.academia.edu/37117740/

[19] Khushboo Sharma, Vinay Sharma, S. S. Sharma., (2018) Dye-Sensitized Solar Cells: Fundamentals and Current Status, Nanoscale Research Letters, Vol.13, 381-427. https://doi.org/10.1186/s11671-018-2760-6

TSCFA 台灣超臨界流體協會
Taiwan Supercritical Fluid Association

(日間班)高壓氣體特定設備操作人員安全衛生教育訓練班

需要有操作證照的單位，歡迎向協會報名。

●上課日期：**111/09/26~09/30 08:00~17:00；09/29~09/30 08:00~17:00(實習)**
●上課時數：高壓氣體特定設備操作人員安全衛生教育訓練課程時數 35 小時＋2 小時(測驗)。
●課程內容：高壓氣體概論 3HR、種類及構造 3HR、附屬裝置及附屬品 3HR、自動檢查與檢點維護 3HR、安全裝置及其使用 3HR、操作要領與異常處理 3HR、事故預防與處置 3HR、安全運轉實習 12HR、高壓氣體特定設備相關法規 2HR，共 35 小時。(另加學科測驗 1 小時及術科測驗約 1~2 小時)
●上課地點：高雄市楠梓區高楠公路 1001 號【金屬工業研究發展中心研發大樓 2 樓　產業人力發展組】
●參加對象：從事高壓氣體特定設備操作人員或主管人員。
●費　　用：本班研習費**新台幣 7,000 元整**，**本會會員享九折優惠**。
●名　　額：每班 30 名，額滿為止。
●結訓資格：期滿經測驗成績合格者，取得【高壓氣體特定設備操作人員安全衛生訓練】之證書。
●報名辦法：1.傳真報名：(07)355-7586台灣超臨界流體協會
2.報名信箱：tscfa@mail.mirdc.org.tw
3.研習費請電匯至 兆豐國際商銀 港都分行(代碼017)
戶名：社團法人台灣超臨界流體協會 帳號：002-09-018479（註明參加班別及服務單位）或以劃線支票抬頭寫「台灣超臨界流體協會」連同報名表掛號郵寄台灣超臨界流體協會，本會於收款後立即開收據寄回。
※洽詢電話：(07)355-5706 吳小姐繳交一吋相片一張及身份證正本

報　　名　　表

課程名稱	高壓氣體特定設備操作人員安全衛生教育訓練			上課日期	111 年 09/26~09/30	
姓　　名	出生年月日	身份證字號	手機號碼	畢業校名		公司產品
服務單位				電　　話		
服務地址	□□□			傳　　真		
發票住址	□□□			統一編號		
負 責 人	人	訓練聯絡人 / 職稱		email：		
參加費用	共　　元	參加性質		□公司指派　　□自行參加		
繳費方式	□郵政劃撥　□支票　□附送現金			報名日期	年　　月　　日	

※ 出生年月日、身份證字號、畢業校名、電話、地址須詳填，以利製作證書。〔！〕

上課日期時間表

課程名稱：(日間班)高壓氣體特定設備操作人員安全衛生教育訓練班

2022/09/26 (一)	08:00 ~ 17:00
2022/09/27 (二)	08:00 ~ 17:00
2022/09/28 (三)	08:00 ~ 17:00
2022/09/29 (四)	08:00 ~ 17:00 (實習第 1 組)
2022/09/30 (五)	08:00 ~ 14:00 (實習第 1 組)

TSCFA 台灣超臨界流體協會
Taiwan Supercritical Fluid Association

(夜間班)高壓氣體特定設備操作人員安全衛生教育訓練班

需要有操作證照的單位，歡迎向協會報名。

●上課日期：**(夜班) 111/10/4~10/14 18:30~21:30；10/15~10/16 08:00~17:00(實習)**

●上課時數：高壓氣體特定設備操作人員安全衛生教育訓練課程時數 35 小時＋2 小時(測驗)。

●課程內容：高壓氣體概論 3HR、種類及構造 3HR、附屬裝置及附屬品 3HR、自動檢查與檢點維護 3HR、安全裝置及其使用 3HR、操作要領與異常處理 3HR、事故預防與處置 3HR、安全運轉實習 12HR、高壓氣體特定設備相關法規 2HR，共 35 小時。(另加學科測驗 1 小時及術科測驗約 1~2 小時)

●上課地點：高雄市楠梓區高楠公路 1001 號【金屬工業研究發展中心研發大樓 2 樓　產業人力發展組】

●參加對象：從事高壓氣體特定設備操作人員或主管人員。

●費　　用：本班研習費**新台幣 7,000 元整**，**本會會員享九折優惠**。

●名　　額：每班 30 名，額滿為止。

●結訓資格：期滿經測驗成績合格者，取得【高壓氣體特定設備操作人員安全衛生訓練】之證書。

●報名辦法：1.傳真報名：(07)355-7586台灣超臨界流體協會
2.報名信箱：tscfa@mail.mirdc.org.tw
3.研習費請電匯至 兆豐國際商銀 港都分行(代碼017)
戶名：社團法人台灣超臨界流體協會 帳號：002-09-018479（註明參加班別及服務單位）或以劃線支票抬頭寫「台灣超臨界流體協會」連同報名表掛號郵寄台灣超臨界流體協會，本會於收款後立即開收據寄回。

※洽詢電話：(07)355-5706 吳小姐繳交一吋相片一張及身份證正本

報　　名　　表

課程名稱	高壓氣體特定設備操作人員安全衛生教育訓練			上課日期	111 年 10/04~10/16	
姓　　名	出生年月日	身份證字號	手機號碼	畢業校名		公司產品
服務單位					電　　話	
服務地址	□□□				傳　　真	
發票住址	□□□				統一編號	
負 責 人	人	訓練聯絡人 / 職稱		email：		
參加費用	共　　元	參加性質		□公司指派　　□自行參加		
繳費方式	□郵政劃撥　□支票　□附送現金			報名日期	年　　月　　日	

※ 出生年月日、身份證字號、畢業校名、電話、地址須詳填，以利製作證書。〔！〕

上課日期時間表

課程名稱：(日間班)高壓氣體特定設備操作人員安全衛生教育訓練班

2022/10/04 (二)	18:30 ~ 21:30
2022/10/05 (三)	18:30 ~ 21:30
2022/10/06 (四)	18:30 ~ 21:30
2022/10/07 (五)	18:30 ~ 21:30
2022/10/11 (二)	18:30 ~ 21:30
2022/10/12 (三)	18:30 ~ 21:30
2022/10/13 (四)	18:30 ~ 21:30
2022/10/14 (五)	18:30 ~ 21:30
2022/10/15 (六)	08:00 ~ 17:00 (實習第 1 組)
2022/10/16 (日)	08:00 ~ 14:00 (實習第 1 組)

SuperGreen2022 國際研討會 10 月 28 日北科大登場

2022/08/01
經濟日報 黃逢森

超臨界流體協會將於 10 月 28 日在集思北科大會議中心舉辦「SuperGreen 2022 國際研討會」，會中將展現我國研發能量及產業發展脈動與國際趨勢互相印證，包括台灣、大陸、日本、韓國等國專業菁英人士與會。

該協會表示，SuperGreen 國際研討會由台灣、日本、中國大陸、韓國發起，每兩年分別在不同國家舉辦會議，2011 年在大陸北京、2013 年在台灣高雄、2015 年在韓國首爾、2017 年在日本京都等，2019 年在大陸西安舉辦，2021 年在台灣舉辦，因疫情延期至 2022 年 10 月。

本屆研討會發表的技術重點為「熱力學與物化性質研究」、「天然物、醫藥與生醫應用」、「反應、材料設計與奈米技」、「製程強化、二氧化碳利用與工業應用」、「超臨界流體於台灣之實務應用」等五大領域，將邀請專家學者作專題演講與論文發表，期能引入新技術應用之觀念及觸發潛在商機。

10 月 28 日、29 日歡迎到集思北科大會議中心，聽演講、學技術、展市場、交朋友、開眼界。學研界的朋友請把握機會，將研發成果與國內產業界分享，投稿截止日期為 8 月 22 日，並於即日起開始接受報名。請參閱研討會網站：https://supergreen2022.conf.tw/。超臨界流體協會網站：https://www.tscfa.org.tw/。超臨界流體協會電話（07）355-5706。

資料來源：https://money.udn.com/money/story/5723/6503962?from=edn_search_result

Development a novel robust method to enhance the solubility of Oxaprozin as nonsteroidal anti-inflammatory drug based on machine-learning

開發一種基於機器學習的新型穩健方法來提高奧沙普秦作為非甾體抗炎藥的溶解度

by **Walid Kamal Abdelbasset**, **Safaa M. Elkholi**, **Khadiga Ahmed Ismail**, **Sameer Alshehri**, **Ahmed Alobaida**, **Bader Huwaimel**, **Ahmed D. Alatawi**, **Amal M. Alsubaiyel**, **Kumar Venkatesan** & **Mohammed A. S. Abourehab**

Department of Health and Rehabilitation Sciences, College of Applied Medical Sciences, Prince Sattam Bin Abdulaziz University, P.O. Box. 173, Al-Kharj, Saudi Arabia

Department of Physical Therapy, Kasr Al-Aini Hospital, Cairo University, Giza, Egypt

Abstract

Accurate specification of the drugs' solubility is known as an important activity to appropriately manage the supercritical impregnation process. Over the last decades, the application of supercritical fluids (SCFs), mainly CO_2, has found great interest as a promising solution to dominate the limitations of traditional methods including high toxicity, difficulty of control, high expense and low stability. Oxaprozin is an efficient off-patent nonsteroidal anti-inflammatory drug (NSAID), which is being extensively used for the pain management of patients suffering from chronic musculoskeletal disorders such as rheumatoid arthritis. In this paper, the prominent purpose of the authors is to predict and consequently optimize the solubility of Oxaprozin inside the CO_2SCF. To do this, the authors employed two basic models and improved them with the Adaboost ensemble method. The base models include Gaussian process regression (GPR) and decision tree (DT). We optimized and evaluated the hyper-parameters of them using standard metrics. Boosted DT has an MAE error rate, an R2-score, and an MAPE of 6.806E-05, 0.980, and 4.511E-01, respectively. Also, boosted GPR has an R2-score of 0.998 and its MAPE error is 3.929E-02, and with MAE it has an error rate of 5.024E-06. So, boosted GPR was chosen as the best model, and the best values were: (T = 3.38E + 02, P = 4.0E + 02, Solubility = 0.001241).

資料來源：https://www.nature.com/articles/s41598-022-17440-4

Numerical Study on Proppant Transport in Supercritical Carbon Dioxide under Different Fracture Shapes: Flat, Wedge-Shaped, and Bifurcated

不同斷口形狀下超臨界二氧化碳中支撐劑輸運的數值研究：平面、楔形和分叉

by **Jiaqiao Xie, Yi Hu***, **Yong Kang**, **Hao Chen**, and **Qi Liu**

School of Power and Mechanical Engineering, Wuhan University, Wuhan 430072, Hubei Province, China

Hubei Key Laboratory of Waterjet Theory and New Technology, Wuhan University, Wuhan 430072, Hubei Province, China

Abstract

As a new type of waterless technology, supercritical carbon dioxide fracturing has been widely studied by scholars in recent years, and the migration characteristics of the corresponding proppant in supercritical carbon dioxide still need further research. In this paper, the Eulerian–Eulerian computational fluid dynamics method was used to study the transport capacity of supercritical carbon dioxide, and the UDF method was used to simulate the physical parameters of supercritical carbon dioxide. In view of the deficiencies of previous studies, the special cases of wedge-shaped fractures and bypass fractures are considered, and the influence of large-span pressure and temperature on migration is first analyzed in plane fractures, which makes this study more complete. The results show that: (1) compared with slickwater, the proppant transport channel in supercritical carbon dioxide is 30% smaller at 305 K and 10 MPa. (2) The transport capacity of supercritical carbon dioxide increases with the increase of pressure and decreases with the increase of temperature. But when the pressure or temperature is too high, they have little effect on it. (3) In wedge-shaped fractures, the proppant stack height and length increase initially as the shrinkage rate of fracture width (the ratio of the fracture reduced width to the fracture length) increases. However, as the fracture width ratio increases, the maximum proppant stack height decreases in the later stage. (4) In bifurcated fractures, with the increase of bypass angle, the area of proppant in the bypass zone tends to decrease. The width of the bypass inlet has little effect on the proppant settlement in the bypass. This study further understands the migration law of proppant in supercritical carbon dioxide in fractures.

資料來源：https://doi.org/10.1021/acs.energyfuels.2c01370

Retention mechanisms of imidazoline and piperazine-related compounds in non-aqueous hydrophilic interaction and supercritical fluid chromatography based on chemometric design and analysis

基於化學計量學設計和分析的咪唑啉和哌嗪相關化合物在非水親水相互作用和超臨界流體色譜中的保留機制

by **D.Obradović[1], Ł.Komsta[2], A.Stavrianidi[34], O.A.Shpigun[3], O.I.Pokrovskiy[5], Z.Vujić[1]**

[1] Department of Pharmaceutical Chemistry, Faculty of Pharmacy, University of Belgrade, Vojvode Stepe 450, 11000 Belgrade, Serbia

[2] Chair and Department of Medical Chemistry, Faculty of Pharmacy, Medical University of Lublin, Jaczwsjiego 4 20-090 Lublin, Poland

[3] Chemistry Department, Lomonosov Moscow State University, 1/3 Leninskie Gory, GSP-1, 119991 Moscow, Russia

[4] A.N. Frumkin Institute of Physical Chemistry and Electrochemistry Russian Academy of Sciences, 31 Leninsky Prospect, GSP-1, 119071 Moscow, Russia

[5] N.S. Kurnakov Institute of General and Inorganic Chemistry of Russian Academy of Sciences, 31 Leninsky Prospect, GSP-1, 119071 Moscow, Russia

Abstract

The experimental design methodology based on central composite design of experiments was applied to compare the retention mechanisms in supercritical fluid chromatography (SFC) and non-aqueous hydrophilic interaction liquid chromatography (NA-HILIC). The selected set consists of 26 compounds that belong to imidazoline and serotonin receptor ligands. The different chemometric tools (multiple linear regression, principal component analysis, parallel factor analysis) were used to examine the retention, as well as to identify the most significant retention mechanisms. The retention mechanism was investigated on two different stationary phases (diol, and mixed-mode diol). In NA-HILIC, the mobile phase contains acetonitrile as a main component, and methanolic solution of ammonium formate (+0.1% of formic acid) as a modifier. The same mobile phase modifier was used in SFC, with a difference in the main component of the mobile phase which was CO_2.

The retention behaviour differs significantly between HILIC and SFC conditions. The retention pattern in HILIC mode was more partition-like, while in SFC the solute-sorbent interactions allowed retention. The retention mechanism between mixed-mode diol and the diol phases varies depending on the applied chromatographic mode, e.g. in HILIC the type of stationary phase significantly affects the elution order, while in SFC this was not the case. The HILIC retention behaviour was influenced by the number of tertiary amines-aliphatic, and N atom-centred fragments in tested compounds. On the other hand, the number of pyrrole and pyridine rings in the structure of the compound showed correlation with their SFC

retention, simultaneously increasing the molecular weight and and rapid elution of larger compounds. It was found that temperature surprisingly plays a major role in SFC mode. The increase in temperature reduces the relative contribution of enthalpy factors to total retention, so the separation in SFC was more entropy-controlled. For further pharmaceutical research and optimization, the SFC would be considered more beneficial compared to HILIC since it gives good selectivity in separation of chosen impurities.

Keywords:Pharmaceutical substances, Chemometric design, Supercritical fluid chromatography, Hydrophilic interaction chromatography

資料來源：https://doi.org/10.1016/j.chroma.2022.463340

SiO_2 synergistic modification of siloxane thickener to improve the viscosity of supercritical CO_2 fracturing fluid

矽氧烷增稠劑 SiO_2 協同改性提高超臨界 CO_2 壓裂液黏度

by Yanling Wang, Bin Liu, Di Li & Lei Liang

a Key Laboratory of Unconventional Oil & Gas Development, Ministry of Education, China University of Petroleum (East China), Qingdao, P. R. China;b School of Petroleum Engineering, China University of Petroleum (East China), Qingdao, P. R. China

Abstract

Supercritical carbon dioxide (SC-CO_2) fracturing technology has the advantages of CO_2 storage and waterless fracturing and has great application potential in the development of unconventional oil and gas resources. However, the low viscosity of SC-CO_2 limits the development of this technology. This paper investigates the synergistic effect of nanomaterials on a developed thickener (HBD-2, high branched D4H). The research results show that among the five micro/nanomaterials Cu-BTC, SiO_2, MCC, MWCNTs, and TiO_2, only SiO_2 has a good synergistic effect on the HBD-2/SC-CO_2 system, and significantly improves its thickening, temperature resistance, temperature resistance and shear resistance. At 60s^{-1}, 305.15 K and 10 MPa, 5 wt.% HBD-2 + 1 wt.% SiO_2 increased the apparent viscosity of SC-CO_2 to 5.82 mPa·s(The viscosity of 5 wt.% HBD-2 under the same conditions is 4.48 mPa·s). The apparent viscosity of SC-CO_2 is positively correlated with pressure and SiO_2 dosage and negatively correlated with temperature and shear rate. The SiO_2/HBD-2 system can effectively avoid clay swelling and can change the water wetness on the core surface to neutral wettability. In addition, we also studied the mechanism of SiO_2 in HBD-2/SC-CO_2 thickening system by RDF(radial distribution function). The results show that the introduction to SiO_2 shifts the peak position of the system to the left and enhances the peak intensity. The macroscopic manifestation is the enhancement of the apparent viscosity of HBD-2/SC-CO_2.This paper proves the feasibility of nanomaterials to synergize SC-CO_2, and provides a new thread for the research and development of SC-CO_2 thickeners in the future.

Keywords: Nanomaterials, supercritical carbon dioxide, thickening, rheology, synergy

資料來源：Energy Sources, Part A: Recovery, Utilization, and Environmental Effects Volume 44, 2022 - Issue 3 https://doi.org/10.1080/15567036.2022.2100946

Study on the Alteration of Pore Parameters of Shale with Different Natural Fractures under Supercritical Carbon Dioxide Seepage

超臨界二氧化碳滲流下不同天然裂縫頁岩孔隙參數變化研究

by **Lei Tao [1,*], Jian Han [2], Yanjun Feng [3] and John D. McLennan [4]**

[1] State Key Laboratory of Oil & Gas Reservoir Geology and Exploitation, Chengdu University of Technology, Chengdu 610059, China

[2] Southwest Oil & Gas Field Company, PetroChina, Chongqing 400707, China

[3] China Coal Technology and Engineering Group Co., Ltd., Coal Mining Research Institute, Beijing 100013, China

[4] Energy and Geoscience Institute, The University of Utah, Salt Lake City, UT 84108, USA

Abstract

Supercritical CO_2 can reduce formation fracture pressure, form more complex fractures in the near-well zone, and replace methane to complete carbon sequestration, which is an important direction for the efficient development of deep shale gas with carbon sequestration. In this paper, based on the $scCO_2$ fracturing field test parameters and the characteristics of common shale calcite filled natural fractures, we simulated the porosity change in shale with three kinds of fractures (no fracture, named NF; axial natural fracture, named AF; and transversal natural fracture, named TF) under $scCO_2$ seepage, and carried out the experimental verification of shale under supercritical CO_2 seepage. It was found that: (1) At the same pressure, when the temperature is greater than the critical temperature, the shale porosity of three kinds of fractures gradually increases with the injection of CO_2, and the higher the temperature, the more obvious the increase in porosity. (2) At the same temperature and different pressures, the effect of pressure change on the porosity of shale specimens was more obvious than that of temperature. (3) Multi-field coupling experiments of shale under supercritical CO_2 seepage revealed that the porosity of all three shale specimens at the same temperature and pressure increased after CO_2 injection, and the relative increase in shale porosity measured experimentally was basically consistent with the numerical simulation results. This paper reveals the mechanism of the effect of different temperatures and pressures of $scCO_2$ and different natural fractures on the change in shale porosity, which can be used to optimize the CO_2 injection in supercritical CO_2 fracturing and carbon sequestration. **View Full-Text**

Keywords: supercritical CO_2; fractured shale; porosity alteration; hydraulic fracturing; carbon sequestration

資料來源：*Minerals* **2022**, *12*(6), 660; https://doi.org/10.3390/min12060660

Supercritical Extraction of a Natural Pyrethrin-Rich Extract from *Chrysanthemum Cinerariifolium* Flowers to Be Impregnated into Polypropylene Films Intended for Agriculture Applications

*菊花*中富含除蟲菊素的天然提取物的超臨界萃取，以浸漬到用於農業應用的聚丙烯薄膜中

by **Claudia Maya** [*], **Casimiro Mantell** [*], **Enrique J. Martínez de la Ossa** and **Lourdes Casas**
Chemical Engineering and Food Technology Department, Wine and Agrifood Research Institute (IVAGRO), University of Cadiz, 11510 Cadiz, Spain

Abstract

The extensive use of synthetic pesticides and their addition to the field presents significant environmental problems that must be minimized. The use of natural insecticides and their addition using techniques that minimize their impact in the field are widely studied by the current scientific community. In this work an extraction method based on supercritical CO_2 to obtain a pyrethrin-rich natural extract from different varieties of chrysanthemum flowers is analyzed. This extract would be used in a supercritical solvent impregnation (SSI) process to produce a commercial polypropylene (PP) film with insecticidal properties to be used in greenhouses. The extract selected for the impregnation process was that obtained from the Atlantis variety at 35 °C and 10 MPa pressure. The amount of insecticide impregnated into the polymer at 55 °C and under two different pressure levels (10 MPa and 40 MPa) have been determined. A batch impregnation method (BM) with 5 h constant impregnation time and low depressurization rates were used to favor the impregnation process. The results demonstrated that this procedure was suitable to produce pyrethrin-loaded PP films that could to be used in greenhouses as a protection against pests, while allowing a more rational and moderate use of other chemical pesticides. **View Full-Text**

Keywords: pyrethrins; supercritical carbon dioxide; polypropylene; supercritical impregnation

資料來源：*AppliedChem* **2022**, *2*(2), 106-116
https://doi.org/10.3390/appliedchem2020007

Supercritical Fluid-Assisted Fabrication of PDA-Coated Poly (L-lactic Acid)/Curcumin Microparticles for Chemo-Photothermal Therapy of Osteosarcoma

超臨界流體輔助製備 PDA 包覆的聚（L-乳酸)/薑黃素微粒用於骨肉瘤的化學光熱治療

by **Zheng Zhao [1,2], Shilu Chen [1], Yao Xiao [1], Maobin Xie [3,4] and Wen Yu [5,*]**

[1] State Key Laboratory of Advanced Technology for Materials Synthesis and Processing, Wuhan University of Technology, Wuhan 430070, China

[2] Sanya Science and Education Innovation Park of Wuhan University of Technology, Sanya 572000, China

[3] Division of Engineering in Medicine, Department of Medicine, Brigham and Women's Hospital, Harvard Medical School, Cambridge, MA 02139, USA

[4] Department of Biomedical Engineering, School of Basic Medical Sciences, Guangzhou Medical University, The Sixth Affiliated Hospital of Guangzhou Medical University, Qingyuan People's Hospital, Guangzhou 511436, China

[5] Affiliated Hospital of Wuhan University of Technology, Wuhan 430070, China

Abstract

After traditional osteosarcoma resection, recurrence of tumor is still a major clinical challenge. The combination of chemotherapy and photothermal therapy (PTT) has great potential in improving therapeutic effect. However, the studies using polydopamine (PDA) as photothermal transducing agent to improve the anti-cancer activity of curcumin (CM)-loaded poly (L-lactic acid) (PLLA) microparticles (PLLA/CM) have seldom been investigated. In this study, we reported the synthesis of PDA-coated PLLA/CM microparticles (PDA-PLLA/CM) prepared by PDA coating on the surface of the PLLA/CM microparticles fabricated by solution-enhanced dispersion by supercritical CO_2 (SEDS) for chemo-photothermal therapy of osteosarcoma. The average particle sizes of PLLA/CM and PDA-PLLA/CM microparticles with a spherical shape were (802.6 ± 8.0) nm and (942.5 ± 39.5) nm, respectively. PDA-PLLA/CM microparticles exhibited pH- and near-infrared (NIR)-responsive release behavior to promote CM release in the drug delivery system. Moreover, PDA-PLLA/CM microparticles displayed good photothermal conversion ability and photothermal stability attributed to PDA coating. Additionally, the results of in vitro anti-cancer experiment showed that 500 μg/mL PDA-PLLA/CM microparticles had good anti-cancer effect on MG-63 cells and no obvious toxicity to MC3T3-E1 cells. After incubation with PDA-PLLA/CM microparticles for 2 days, NIR irradiation treatment improved the anti-cancer activity of PDA-PLLA/CM microparticles obviously and reduced the cell viability of osteosarcoma from 47.4% to 20.6%. These results indicated that PDA-PLLA/CM microparticles possessed a synergetic chemo-photothermal therapy for osteosarcoma. Therefore, this study demonstrated

that PDA-PLLA/CM microparticles may be an excellent drug delivery platform for chemo-photothermal therapy of tumors. **View Full-Text**

Keywords: osteosarcoma therapy; microparticles; curcumin; synergetic chemo-photothermal therapy

資料來源：*Coatings* **2022**, *12*(4), 524; https://doi.org/10.3390/coatings12040524